CHEMBIOCHEM

Supporting Information

DOI: 10.1002/cbic.200900584

Supporting Information

for

Exploring the Substrate Promiscuity of Drug-modifying Enzymes for the Chemoenzymatic Generation of *N*-Acylated Aminoglycosides

Keith D. Green, Wenjing Chen, Jacob L. Houghton,
Micha Fridman*, and Sylvie Garneau-Tsodikova*

Bacterial strains, plasmids, materials, and instrumentation: Chemically competent *E. coli* TOP10 and BL21 (DE3) were bought from Invitrogen. Restriction endonucleases, T4 DNA ligase, and Phusion DNA polymerase were purchased from NEB. DNA primers for PCR were purchased from Integrated DNA Technologies. The pET28a and pET22b vectors were purchased from Novagen. The Int-pET19b-pps containing a decahistidine tag separated from the gene by PreScission protease was generously provided by Dr. Tapan Biswas (Univeristy of Michigan, MI, USA).[1] Precision protease was purchased from GE Healthcare (Piscataway, NJ, USA). DNA sequencing was performed at the University of Michigan DNA sequencing Core. DTDP, commercially available CoA derivatives (acetoacetyl-CoA, acetyl-CoA, benzoyl-CoA, butyryl-CoA, crotonyl-CoA, glutaryl-CoA, D,L-β-hydroxybutyryl-CoA, isovaleryl-CoA, malonyl-CoA, methylmalonyl-CoA, palmitoyl-CoA, *n*-propionyl-CoA,) and aminoglycosides (amikacin, gentamicin, kanamycin A, neomycin B, paromomycin, sisomicin, and tobramycin) were purchased from Sigma-Aldrich and used without any further purification. ThioGlo-1 (TG1) was bought from Calbiochem. Determination of kinetic parameters by UV-Vis assays was done on a multimode SpectraMax M5 plate reader by using 96-well plates (Fisher Scientific). Fast protein liquid chromatography (FPLC) was performed as the last protein purification step on a Bio-Rad BioLogic DuoFlow using a HighPrep^{TM} 26/60 Sephacryl^{TM} S-200 High Resolution column.

Methods:

Preparation of pAAC(6')-APH(2")-pET28a, pAAC(6')-APH(2")-pET22b, pAAC(6')-APH(2")-Int-pET19b-pps, pAAC(3)-IV-pET28a, and pAAC(3)-IV-Int-pET19b-pps Overexpression Constructs. The gene encoding AAC(6')-APH(2") was PCR-amplified using the vector pSF815 in which the gene was stored as a template (provided by Prof. Timor Baasov, Israel Institute of Technology) and Phusion High-Fidelity DNA polymerase. The gene encoding AAC(3)-IV was PCR-amplified using plasmid DNA pAAC(3)-IV-pET23a (a gift from Dr. John S. Blanchard, Albert Einstein College of Medicine, NY). The primers used for the amplification of each gene are listed in Table S1. The amplified genes were inserted into the linearized pET28a, pET22b, and Int-pET19b-pps vectors via the corresponding *Nde*I/*Xho*I (pAAC(6')-APH(2")-pET28a-(NHis), pAAC(6')-APH(2")-pET22b(CHis), and pAAC(6')-APH(2")-Int-pET19b-pps-(NHis)), *Nde*I/*Hind*III (pAAC(3)-IV-pET28a(NHis)), and *Nde*I/*Bam*HI (pAAC(3)-IV-Int-pET19b-pps(NHis)) restriction sites, to afford constructs that encode for NHis-tagged and CHis-tagged proteins. The Int-pET19b-pps vector was utilized to produce proteins with an easily cleavable NHis-tag by use of precision protease. Expression of AAC(6')-APH(2")-pET28a(NHis), AAC(6')-APH(2")-pET22b(CHis), AAC(6')-APH(2")-Int-pET19b-pps(NHis), AAC(3)-IV-pET28a(NHis), and AAC(3)-IV-Int-pET19b-pps-(NHis) was done following transformation into *E. coli* TOP10 competent cells. The plasmids were sequenced (The University of Michigan DNA Sequencing Core) and showed perfect alignment with the reported sequences (PubMed accession number NC_002774 for AAC(6')-APH(2") and PubMed accession number DQ241380 for AAC(3)-IV).

Table S1. Primers used for the PCR amplification of the AAC(6')-APH(2") gene from *S. aureus* and the AAC(3)-IV gene from *E. coli*.

gene (vector used for cloning)	5' primer	3' primer
aac(3)-IV(NHis) (pET28a)	ACATATGCAATACGAATGGC GAAAAGCC	GTGGGCAAGCTTTCAGCCAATCGACTGG CGAGCGG
aac(3)-IV(NHis) (Int-pET19b-pps)	ACATATGCAATACGAATGGC GAAAAGCC	GTGGGCGGATCCTCAGCCAATCGACTGG CGAGCGG
aac(6')-aph(2")(NHis) (pET28a and Int-pET19b-pps)	GATAAACATATGAATATAGT TGAAAATGAAATATG	TATATTCTCGAGTCAATCTTTATAAGTC CTTTTATAAATTTC
aac(6')-aph(2")(CHis) (pET22b)	GATAAACATATGAATATAGT TGAAAATGAAATATG	ATTATACTCGAGATCTTTATAAGTCCTTT TATAAATTTC

The introduced restriction sites are underlined for each primer. The 5' primers all introduced an NdeI restriction site. The 3' primer for aac(3)-IV(NHis) (pET28a), aac(3)-IV(NHis) (Int-pET19b-pps), and all aac(6')-aph(2") introduced HindIII, BamHI, and XhoI restriction sites, respectively.

The tags added to the proteins are:

NHis (pET28a/*Nde*I) = MGSSHHHHHHSSGLVPRGSH

NHis (Int-pET19b-pps/*Nde*I) = MGHHHHHHHHHHSSGHINNNNKHTSLEVLFQGPH

No tag (after cleavage using precision protease and Int-pET19b-pps/*Nde*I) = GPH

CHis (pET22b/*Xho*I) = LEHHHHHH

CHis (pET22b/*Hind*III) = KLAALEHHHHHH

Overproduction and Purification of AAC(6')-APH(2")(NHis), AAC(6')-APH(2")-(CHis), and AAC(3)-IV(NHis). Purified plasmids AAC(6')-APH(2")-pET28a(NHis), AAC(6')-APH(2")-pET22b(CHis), AAC(6')-APH(2")-Int-pET19b-pps(NHis), AAC(3)-IV-pET28a(NHis), and AAC(3)-IV-Int-pET19b-pps(NHis) were transformed into *E. coli* BL21 (DE3) competent cells for protein expression and purification. 1 L of Luria-Bertani (LB) medium supplemented with kanamycin (50 μg/mL) (for pET28a constructs) or ampicillin (100 μg/mL) (for pET22b and Int-pET19b-pps constructs) were inoculated with 10 mL of an overnight culture of the transformants harboring the AAC(6')-APH(2")-pET28a, AAC(6')-APH(2")-pET22b, AAC(6')-APH(2")-Int-pET19b-pps, AAC(3)-IV-pET28a, and AAC(3)-IV-Int-pET19b-pps constructs and incubated at 37 °C. The cultures were grown to an OD_{600} of ~0.6, induced with 1 mL of a 1 M stock of isopropryl-β-thiogalactopyranoside (IPTG) (final concentration of 1.0 mM) and shaken for an additional 4 h at 37 °C. Cells were harvested by centrifugation (6000 rpm, 10 min, 4 °C, Beckman Coulter Aventi JE centrifuge, F10 rotor) and resuspended in buffer A [300 mM NaCl and 50 mM Na_2HPO_4 pH 8.0 adjusted at RT, (containing 10%

glycerol for the AAC(3)-IV proteins)]. Resuspended cells were lysed (1 pass at 10 000-15 000 psi, Avestin EmulsiFlex-C3 high-pressure homogenizer), and the cell debris was removed by centrifugation (16 000 rpm, 45 min, 4 °C, Beckman Beckman Coulter Aventi JE centrifuge, JA-17 rotor). Imidazole (final concentration of 2 mM) was added to the supernatant, which was then incubated with 2 mL of Ni-NTA agarose resin (Qiagen) at 4 °C for 2 h with gentle rocking. The resin was loaded onto a column and washed with 10 mL of buffer A containing 5 mM imidazole and with 10 mL of buffer A containing 20 mM imidazole. The desired protein was eluted from the column in a stepwise imidazole gradient (10 mL fraction of 20 mM (1x), 5 mL fractions of 20 mM (3x), 40 mM (3x), and 250 mM imidazole (3x)). Fractions containing the pure desired proteins [as determined by sodium dodecyl sulfate-polyacrylamide gel electrophoresis (SDS-PAGE)] were combined and dialyzed at 4 °C against 1 L of buffer B [50 mM HEPES, pH 7.5 adjusted at RT] for 3 h. The dialyzed proteins were either further purified on FPLC (1.5 mL/min using buffer C [50 mM HEPES, pH 7.5 adjusted at RT]) or treated with precision protease to cleave the NHis tag from the proteins produced using the Int-pET19b-pps vector (see protocol in the next section) (Figures S1, S3, and S4). Pure proteins were concentrated using Amicon Ultra PL-10. Protein concentrations were determined using a Nanodrop spectrometer (Thermo Scientific). Protein yields were 1.3-5.1 mg per L of culture for all AAC(6')-APH(2") and 3-22 mg per L of culture of all AAC(3)-IV. All AAC(6')-APH(2") proteins were stored at 4 °C while all AAC(3)-IV proteins were flash-frozen (with 10% glycerol added to the protein) using liquid nitrogen and stored at -80 °C.

Cleavage of NHis Tag from AAC(6')-APH(2") Produced from the Int-pET19b-pps Construct. The NHis tag was cleaved overnight at 4 °C with rocking using 30 µg of PreScission protease in 50 mM HEPES (pH 7.5 adjusted at RT). The protein was loaded on 15% SDS-PAGE gel to verify that the tag was completely removed. If cleavage was incomplete, an additional 30 µg of precision protease was added and rocked at RT for an additional 3-6 h. The cleavage progress was checked again by SDS-PAGE gel and if incomplete, the remaining tagged protein was separated from the untagged by binding to Ni-NTA agarose beads. The flow-through was collected and purified by FPLC (1.5 mL/min using buffer C [50 mM HEPES, pH 7.5 adjusted at RT]).

pH Profile of AAC(6')-APH(2")(NHis) and AAC(3)-IV(NHis) Purified from pET28a. The pH profile of AAC(6')-APH(2")(NHis) and AAC(3)-IV(NHis) purified from pET28a were determined for each aminoglycoside substrate (200 μL reaction volume) by monitoring CoA-SH, released due to acylation, reacting with 4,4'-dithiodipyridine which gives an increase in absorbance at 324 nm (ε_{324} = 19 800 $M^{-1}cm^{-1}$)[2] due to the formation of 4-thiopyridone, using acetyl-CoA (40 μM), DTDP (2 mM), and aminoglycoside (20 μM) in the various buffers (50 mM). A pH range from 4.5 to 9.0 using 0.3 increments was used to determine the optimum pH of the AACs activity with individual sugars. Citrate-phosphate buffer (50 mM) was used for pHs 4.5 to 5.4, MES (50 mM) was used for pHs 5.7 to 6.6, HEPES (50 mM) for pHs 6.9 to 7.8, and Tris (50 mM) for pHs 8.1 to 9.0. Data were recorded every 30 s for 15 to 30 min. The rate of each reaction was determined using the initial slope (in the first 2.5 min), and plotted versus the pH (Figure S5). Plots generally indicated one optimum pH or a small range of pHs.

Determination of CoA Derivatives Substrate Specificity for AAC(6')-APH(2")-(NHis) and AAC(3)-IV(NHis) from pET28a. To determine which CoA derivatives are substrates for AAC(6')-APH(2")(NHis) and AAC(3)-IV(NHis) from pET28a, the acylation of the aminogylcosides were monitored using the same spectrophotometric assay as above. Reaction volumes of 200 μL contained buffer (50 mM) [MES pH 6.6 for the AAC(6')-APH(2") enzyme for all aminoglycosides, MES pH 6.6 for the AAC(3)-IV enzyme for paromomycin and tobramycin, and MES pH 5.7 for AAC(3)-IV enzymes for gentamicin, sisomicin, and neomycin B], DTDP (2 mM), CoA derivatives (40 μM), and aminogylcoside (20 μM). The reactions were initiated using 5.9 μg of protein. Solutions were pre-incubated at 37 °C for 5 min prior to addition of enzyme. The enzymatic reactions were monitored by taking readings every 30 s for 30 min (Figures S6-S10).

Determination of Kinetic Paramaters. The kinetic parameters for each enzyme were determined in reactions (200 μL) containing 0-80 μM of CoA derivatives (0, 1, 2, 3, 4, 5, 6, 10, 20, 30, 40, 80 μM) (higher concentrations, up to 1 mM, were used in cases that revealed a K_m higher than 80 μM), aminoglycoside (100 μM), DTDP (2 mM), and enzyme (0.25 μM) at the optimum pH for individual aminoglycosides as determined by the pH profile (i.e. the pH giving the fastest rate). Reactions were initiated by the addition of the CoA derivatives and were carried out in triplicate. The kinetic parameters, K_m and k_{cat} were determined using Lineweaver-Burke plots (Figures

S11-S13). The determination of kinetic parameters using ThioGlo-1 (TG1) was done identically, only using TG1 (100 μM) in place of DTDP.

TLC Time Course. Reactions (100 μL) were carried out at 37 ℃ (AAC(6')-APH(2")) or at RT (AAC(3)-IV) in MES (50 mM, pH 6.6 adjusted at RT) (neomycin B) or at RT in MES (50 mM, pH 5.7 adjusted at RT) (gentamicin) in the presence of CoA derivative (200 μM), aminoglycoside (150 μM), and AAC (5-6 μM). Aliquots (~5 μL) were loaded on a TLC plate (EMD, Silica gel F254 250 μm tickness) after 0, 10, 30, 60, 120, 300 min, and overnight incubation. The eluent systems utilized were MeOH/NH_4OH 3:2 (neomycin B) and 6:1/MeOH:NH_4OH (gentamicin). Visualization was achieved by using a cerium-molybdate stain (5 g CAN, 120 g ammonium molybdate, 80 mL H_2SO_4, 720 mL H_2O). The R_f values observed were 0.23 for neomycin B; 0.43 for 6'-*N*-acetyl-neomycin B; 0.47 for 6'-*N*-*n*-propionyl-neomycin B; 0.31 for 3-*N*-acetyl-neomycin B; 0.42 for 3-*N*-*n*-propionyl-neomycin B; 0.10 for gentamicin; 0.20 for 3-*N*-acetyl-gentamicin; 0.27 for 3-*N*-*n*-propionyl-gentamicin Starting materials and by-product were visualized by TLC to determine their R_f values using the appropriate eluent systems (Figure S14).

TLC time course for double acetylation of neomycin B. Reactions (100 μL) were carried out at 37 ℃ (for AAC(6')-APH(2")) or at RT (for AAC(3)-IV) in MES (50 mM, pH 5.7 adjusted at RT) in the presence of acetyl-CoA (600 μM), aminoglycoside (150 μM), and AAC (6 μM) for 1 h. The second AAC was added to the mixture and the reaction was incubated for an additional 1 h. Aliquots (5 μL) of each reaction were loaded onto a TLC plate (EMD, Silica gel F254 250 μm tickness). The eluent systems utilized were MeOH/NH_4OH 3:2 and visualization was achieved by using a cerium-molybdate stain (5 g CAN, 120 g ammonium molybdate, 80 mL H_2SO_4, 720 mL H_2O). The R_f values observed were 0.46 for 6',3-*N*-diacetyl-neomycin B.

BioTLC. Reactions (10-20 μL) were inspired by the work of Ostash et al.[3] and were carried out in MES (50 mM, pH 6.6 adjusted at RT) for AAC(6')-APH(2") (0.7 nmol) or MES (50 mM, pH 5.7 adjusted at RT) for AAC(3)-IV (0.5 nmol) in the presence of CoA derivative (40-80 nmol), aminoglycoside (neomycin B, gentamicin) (30-60 nmol). After completion of the reaction (monitored by TLC), an equal volume of MeOH was added to precipitate the protein. The solutions were centrifuged (14 000 rpm, 10 min, RT) to pellet the protein. The entire reaction mixture was loaded onto a TLC plate and ran in the aforementioned eluent systems. A small amount of the reaction was

stained with a cerium-molybdate stain prior to loading on the BioTLC to check for reaction completion. *Bacillus subtilis* was grown in LB (no antibiotic) at 30 ℃ for a 24 h period. The bacterial culture (100 µL) was added to soft agar (0.75%) LB (10 mL) at 37 ℃ and poured over the TLC plate in a sterile pe tri dish. The *B. subtilis* overlay was grown until clear zones of inhibited growth were observed (10 h – overnight) at 30 ℃. The R_f values of the starting materials and products on the stained TLCs corresponded to the R_f values of the zones of inhibition on the overlay.

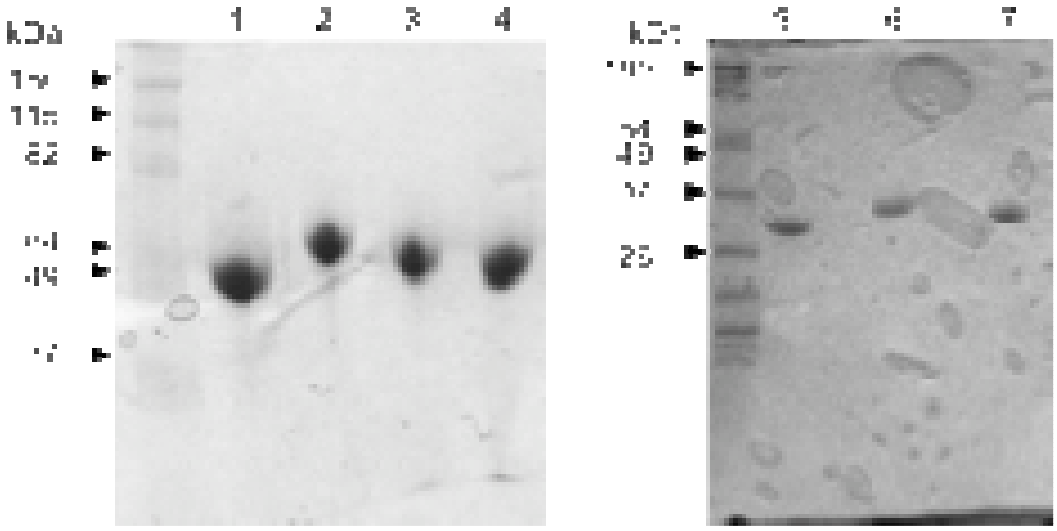

Figure S1. Coomassie blue-stained 15% Tris-HCl SDS-PAGE gel showing the purified AAC(6')-APH(2")(no tag) (Int-pET19b-pps) (56992 Da, lane 1), AAC(6')-APH(2")(NHis) (Int-pET19b-pps) (60897 Da, lane 2), AAC(6')-APH(2")(NHis) (pET28a) (59155 Da, lane 3), AAC(6')-APH(2")(CHis) (pET22b) (57678 Da, lane 4), AAC(3)-IV(no tag) (Int-pET19b-pps) (27906 Da, lane 5), AAC(3)-IV(NHis) (Int-pET19b-pps) (31882 Da, lane 6), and AAC(3)-IV(NHis) (pET28a) (30069 Da, lane 7). 6 µg of each protein were loaded on the gel.

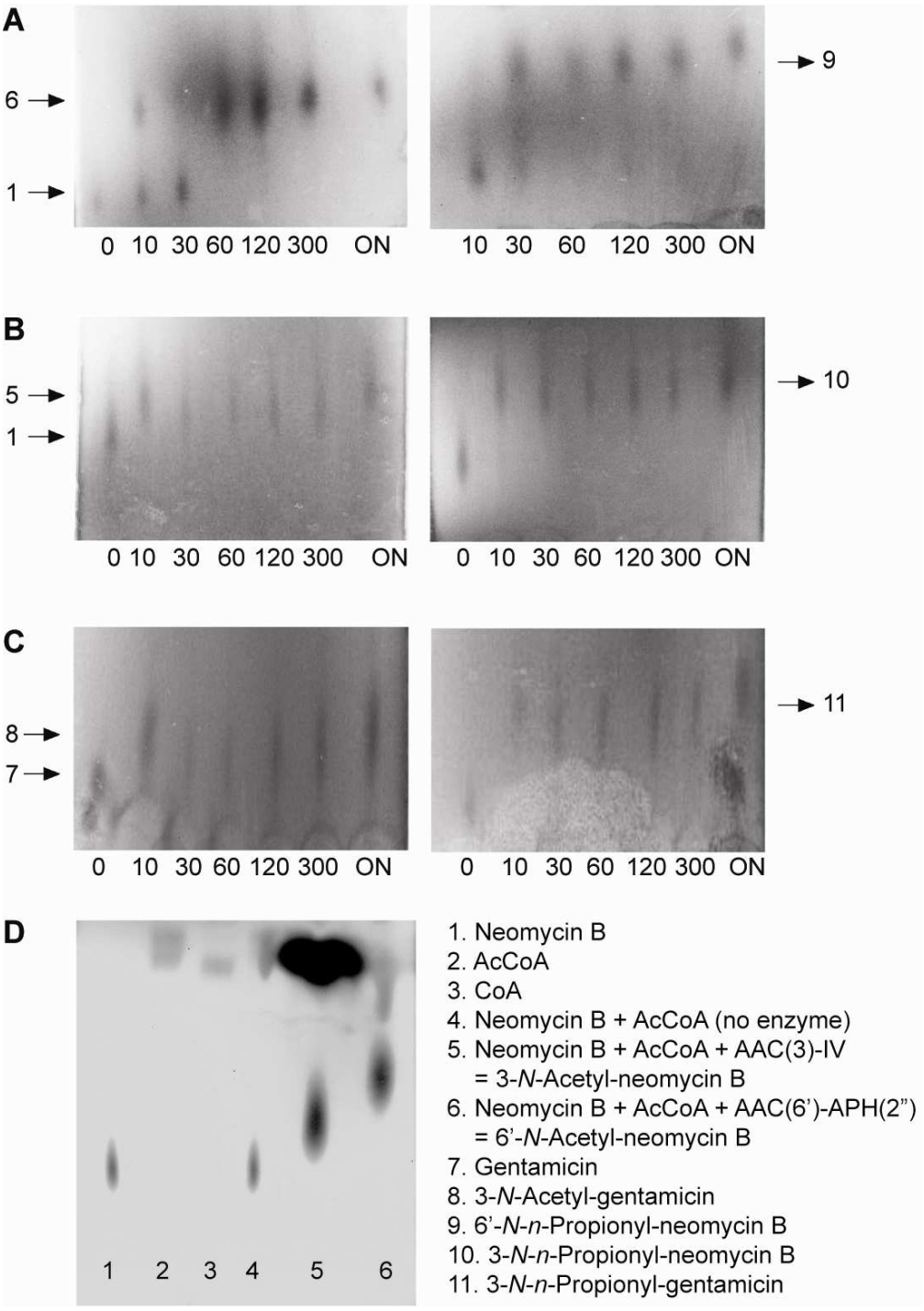

Figure S2. TLC time courses using acetyl-CoA or *n*-propionyl-CoA of the **A.** AAC(6')-APH(2") reactions with neomycin B showing the formation of 6'-*N*-acetyl-neomycin B and 6'-*N*-*n*-propionyl-neomycin B, **B.** AAC(3)-IV reaction with neomycin B showing the formation of 3-*N*-acetyl-neomycin B and 3-*N*-*n*-propionyl-neomycin B, and **C.** AAC(3)-IV reaction with gentamicin showing the formation of 3-*N*-acetyl-gentamicin and 3-*N*-*n*-propionyl-gentamicin. **D.** Control TLC showing that without an AAC enzyme the substrate remains unchanged, whereas with AACs the substrate gets acylated.

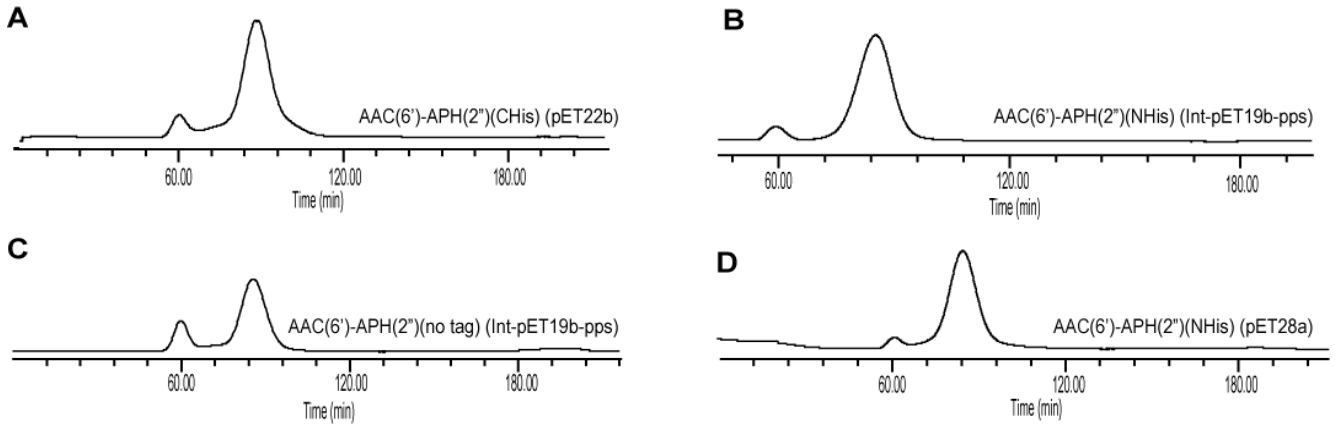

Figure S3. FPLC traces observed at 280 nm for **A** AAC(6')-APH(2")(CHis) (pET22b), **B** AAC(6')-APH(2")(NHis) (Int-pET19b-pps), **C** AAC(6')-APH(2")(no tag) (Int-pET19b-pps), and **D** AAC(6')-APH(2")(NHis) (pET28a).

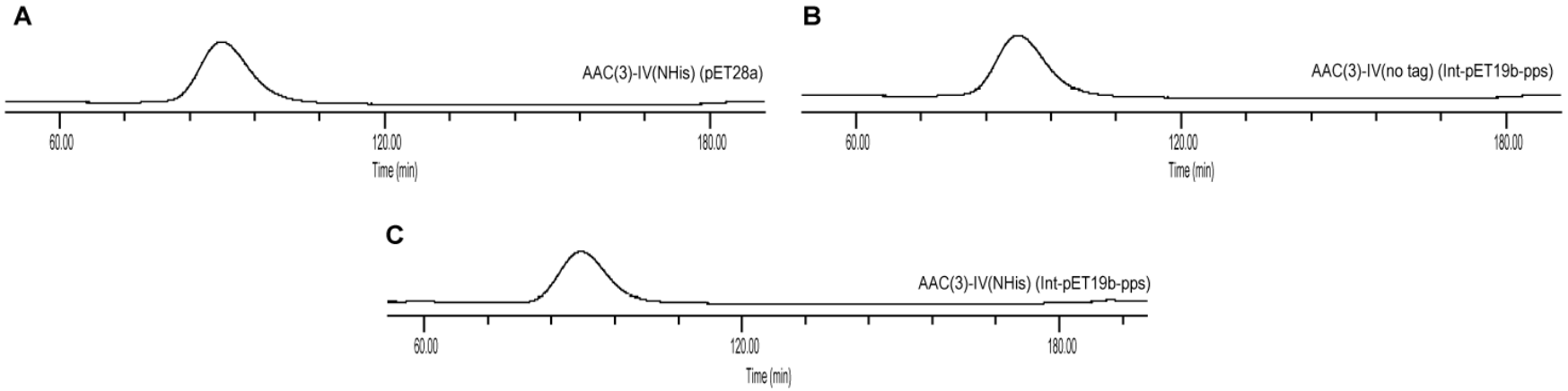

Figure S4. FPLC traces observed at 280 nm for **A.** AAC(3)-IV(NHis) (pET28a), **B.** AAC(3)-IV(no tag) (Int-pET19b-pps), and **C.** AAC(3)-IV(NHis) (Int-pET19b-pps).

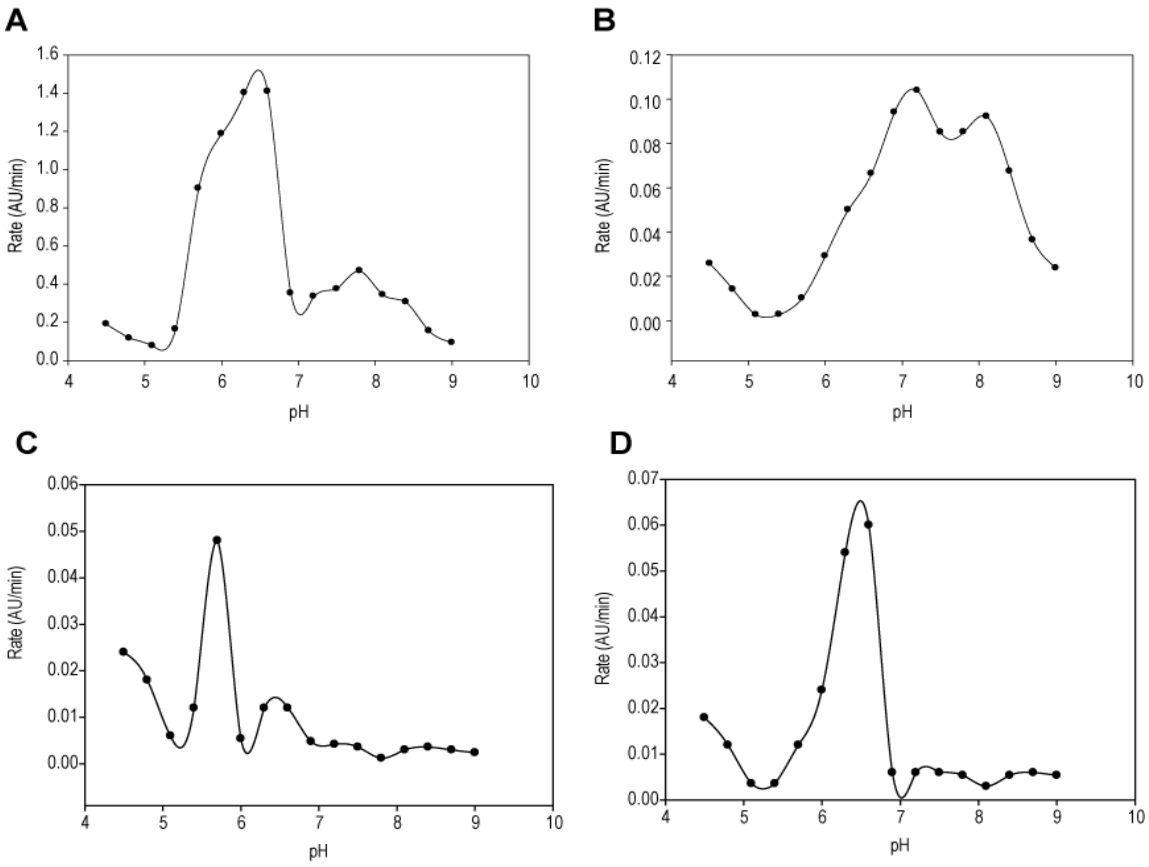

Figure S5. Representative pH profiles for **A** kanamycin A with AAC(6')-APH(2")(NHis) (pET28a), **B** sisomicin with AAC(6')-APH(2")(NHis) (pET28a), **C** sisomicin with AAC(3)-IV(NHis) (pET28a), and **D** paromomycin with AAC(3)-IV(NHis) (pET28a).

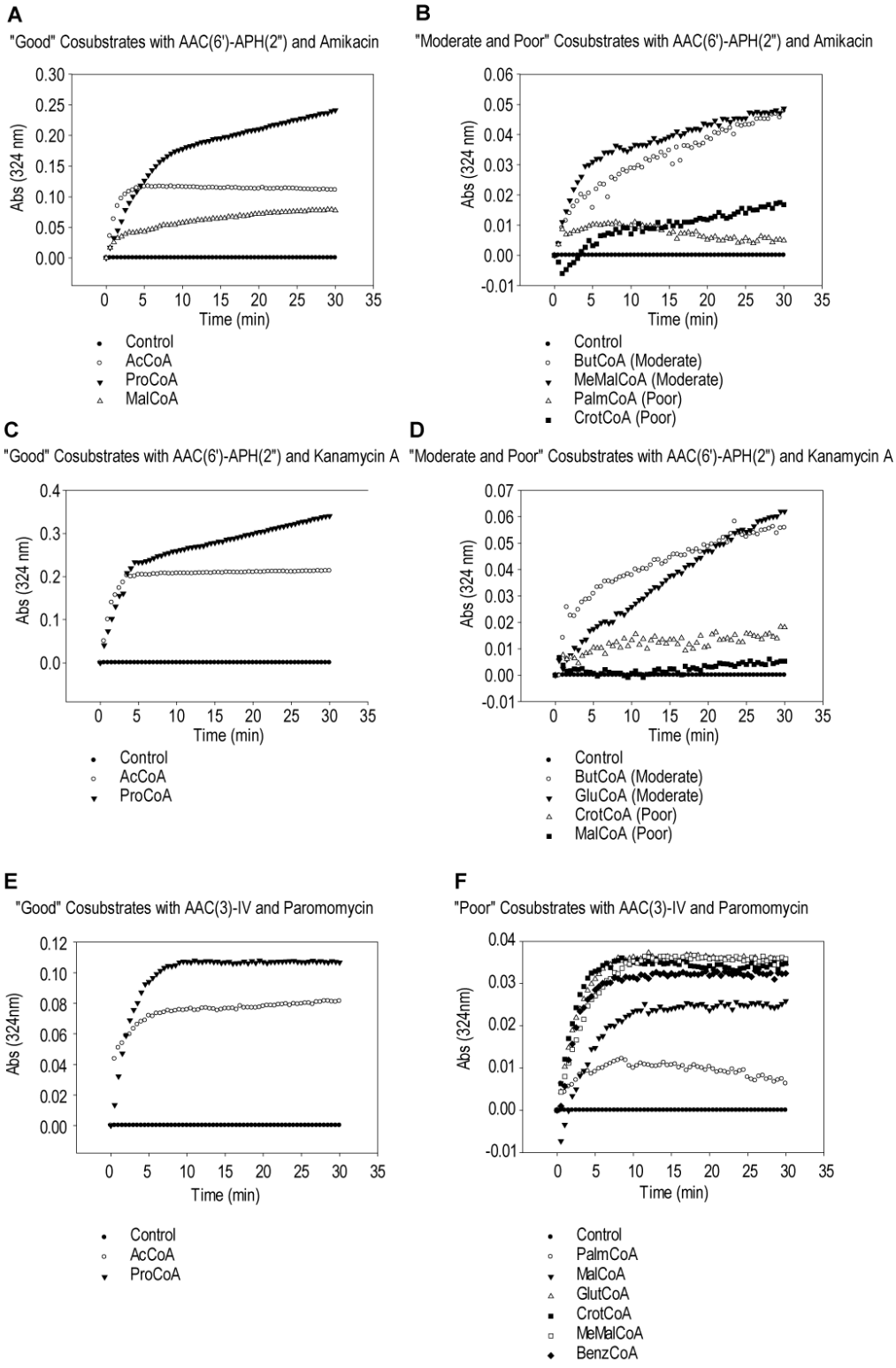

Figure S6. Representative spectrophotometric assay plots of **A.** "good" substrates with amikacin and AAC(6')-APH(2")(NHis) (pET28a), **B.** "moderate and poor" substrates with amikacin and AAC(6')-APH(2")(NHis) (pET28a), **C.** "good" substrates with kanamycin A and AAC(6')-APH(2")(NHis) (pET28a), **D.** "moderate and poor" substrates with kanamycin A and AAC(6')-APH(2")(NHis) (pET28a), **E.** "good" substrates with paromomycin and AAC(3)-IV(NHis) (pET28a), and **F.** "poor" substrates with paromomycin and AAC(3)-IV(NHis) (pET28a).

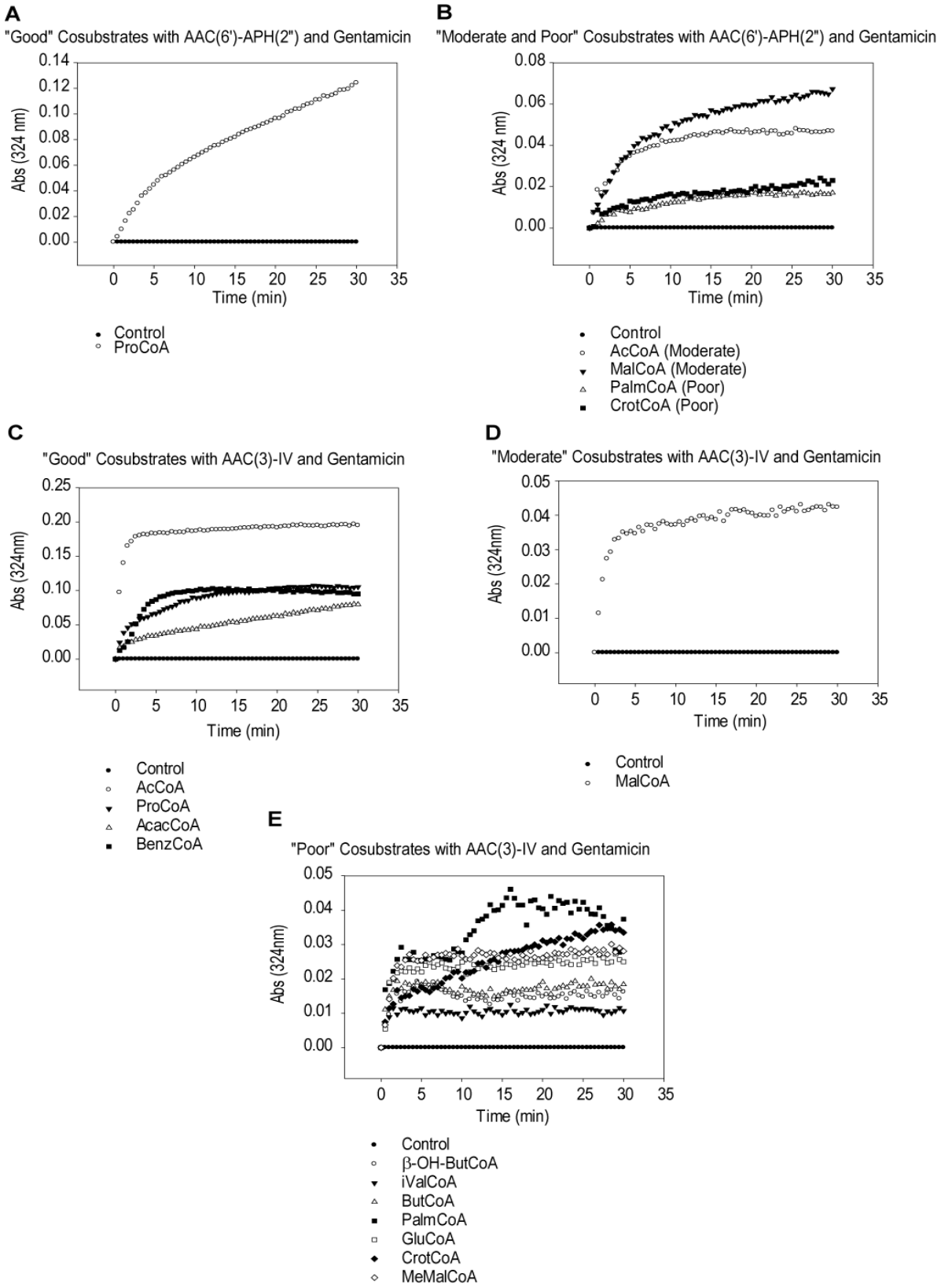

Figure S7. Representative spectrophotometric assay plots of **A.** “good” substrates with gentamicin and AAC(6’)-APH(2”)(NHis) (pET28a), **B.** “moderate and poor” substrates with gentamicin and AAC(6’)-APH(2”)(NHis) (pET28a), **C.** “good” substrates with gentamicin and AAC(3)-IV(NHis) (pET28a), **D.** “poor” substrates with gentamicin and AAC(3)-IV(NHis) (pET28a), and **E.** “poor” substrates with gentamicin and AAC(3)-IV(NHis) (pET28a).

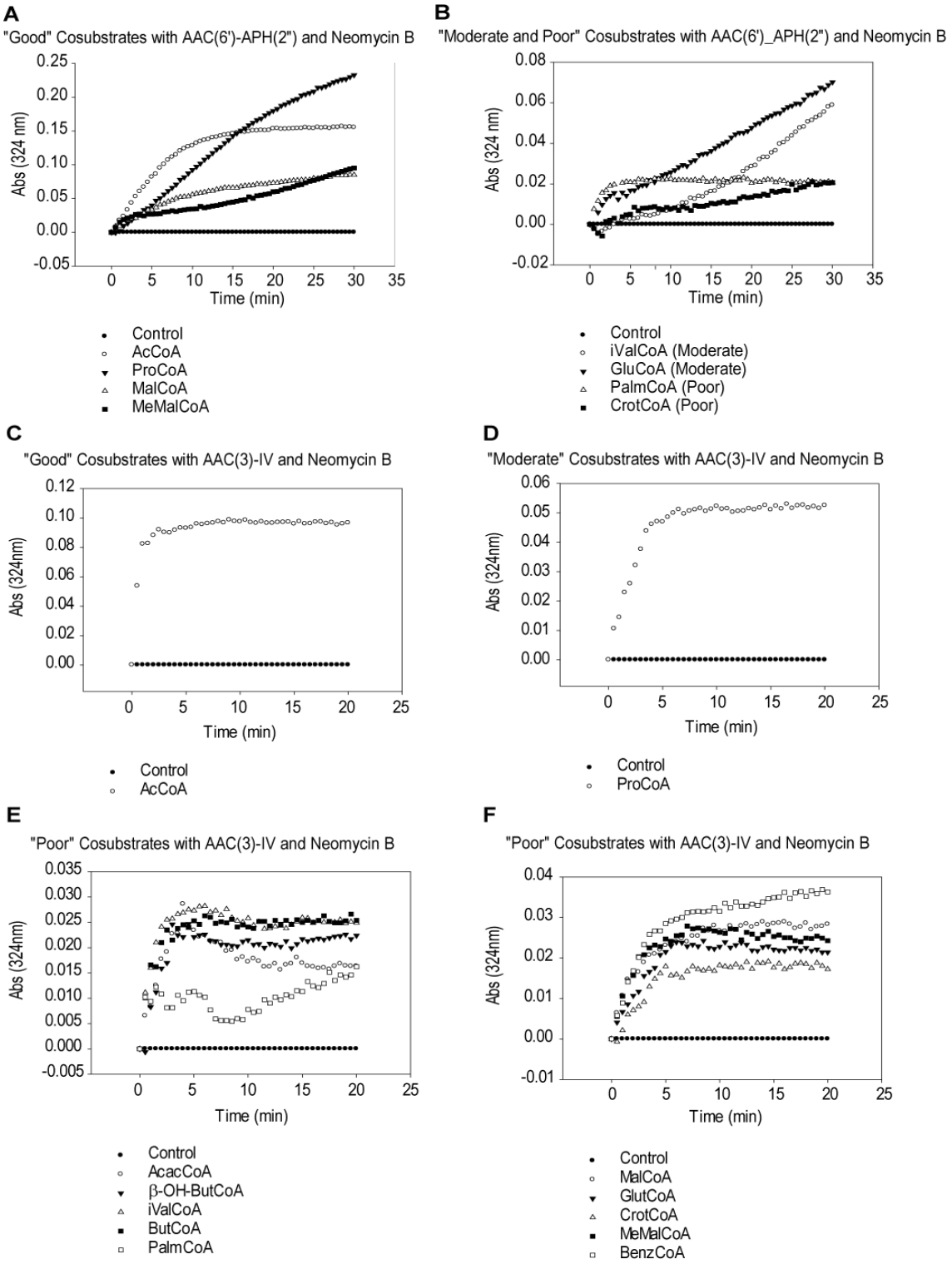

Figure S8. Representative spectrophotometric assay plots of **A.** “good” substrates with neomycin B and AAC(6’)-APH(2”)(NHis) (pET28a), **B.** “moderate and poor” substrates with neomycin and AAC(6’)-APH(2”)(NHis) (pET28a), **C.** “good” substrates with neomycin B and AAC(3)-IV(NHis) (pET28a), **D.** “moderate” substrates with neomycin B and AAC(3)-IV(NHis) (pET28a), **E.** “poor” substrates with neomycin B and AAC(3)-IV(NHis) (pET28a), and **F.** “poor” substrates with neomycin B and AAC(3)-IV(NHis) (pET28a).

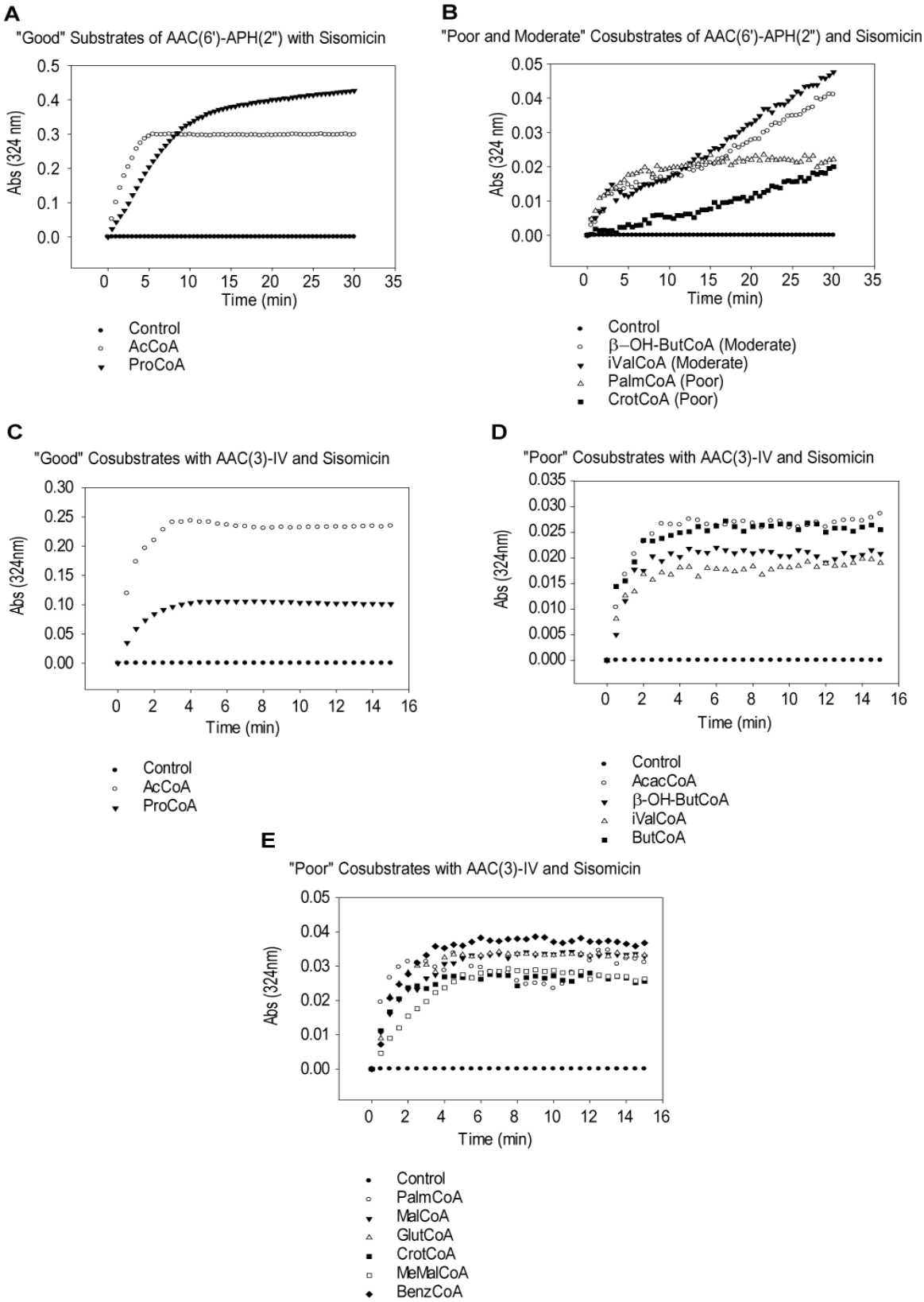

Figure S9. Representative spectrophotometric assay plots of **A.** “good” substrates with sisomicin and AAC(6’)-APH(2”)(NHis) (pET28a), **B.** “moderate and poor” substrates with sisomicin and AAC(6’)-APH(2”)(NHis) (pET28a), **C.** “good” substrates with sisomicin and AAC(3)-IV(NHis) (pET28a), **D.** “poor” substrates with sisomicin and AAC(3)-IV(NHis) (pET28a), and **D.** “poor” substrates with sisomicin and AAC(3)-IV(NHis) (pET28a).

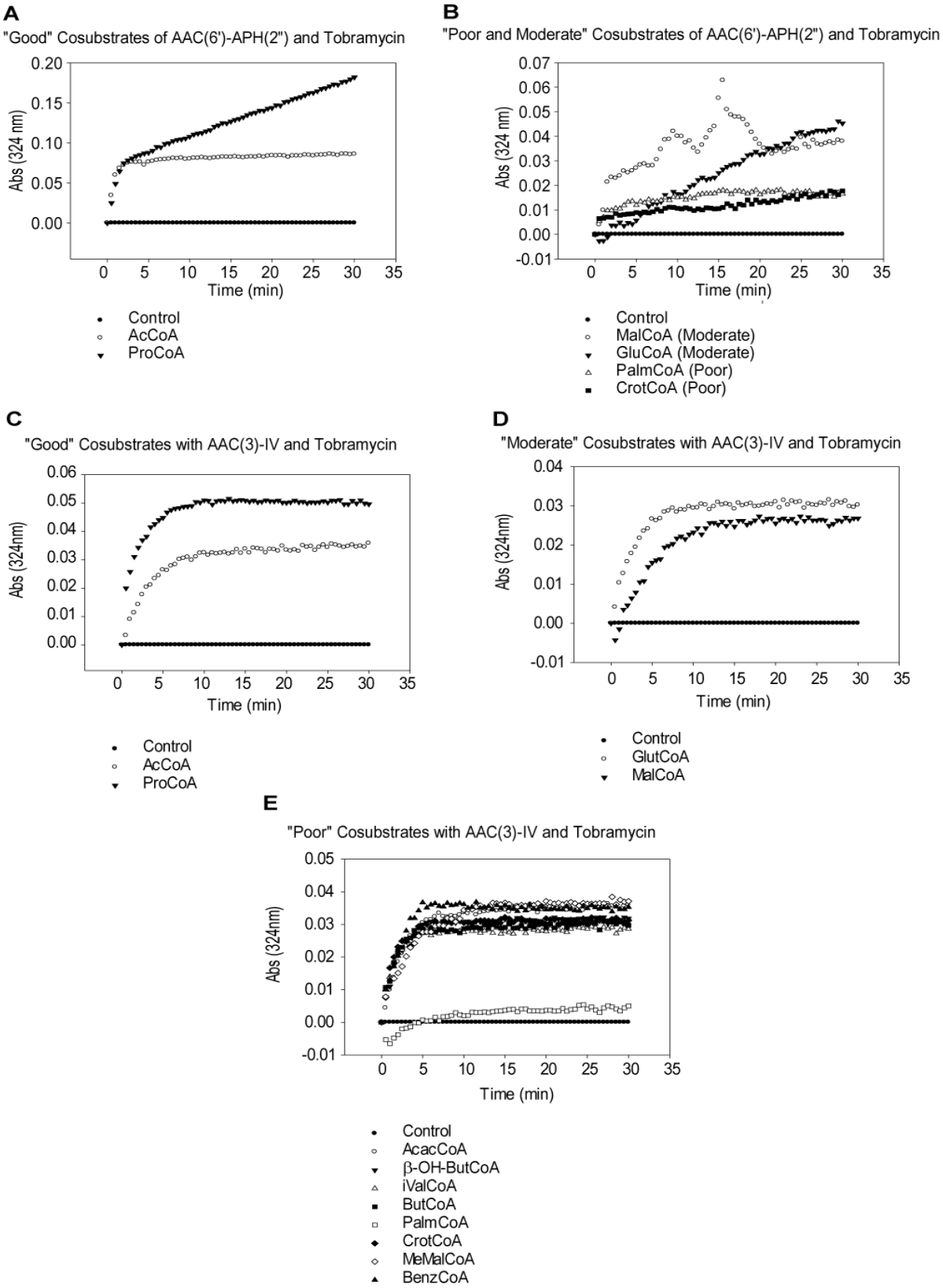

Figure S10. Representative spectrophotometric assay plots of **A.** “good” substrates with tobramycin and AAC(6’)-APH(2”)(NHis) (pET28a), **B.** “moderate and poor” substrates with tobramycin and AAC(6’)-APH(2”)(NHis) (pET28a), **C.** “good” substrates with tobramycin and AAC(3)-IV(NHis) (pET28a), **D.** “poor” substrates with tobramycin and AAC(3)-IV(NHis) (pET28a), and **E.** “poor” substrates with tobramycin and AAC(3)-IV(NHis) (pET28a).

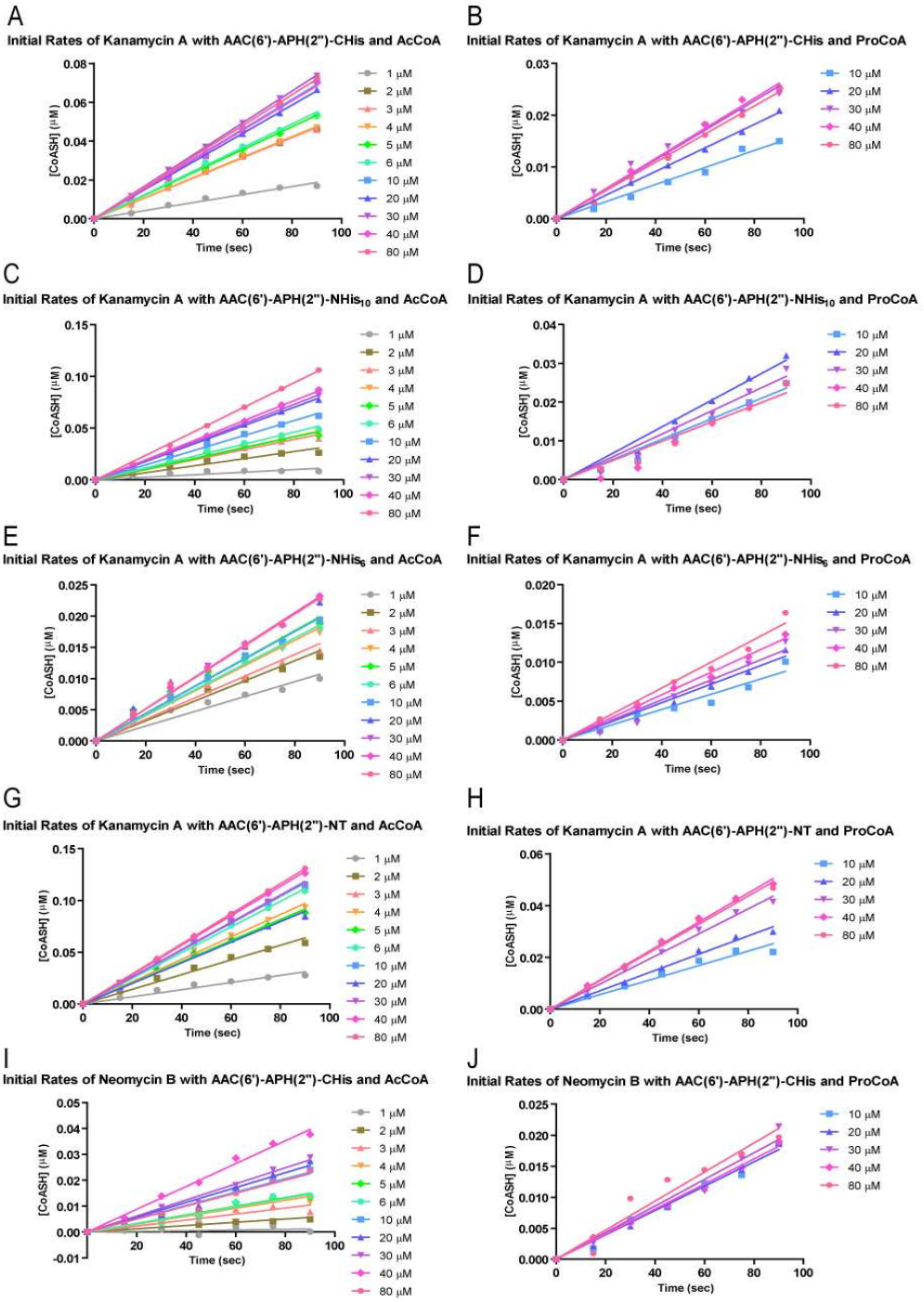

Figure S11. Example kinetic initial rates of **A.** kanamycin A with AAC(6')-APH(2")(CHis) (pET22b) and acetyl-CoA, **B.** kanamycin A with AAC(6')-APH(2")(CHis) (pET22b) and *n*-propionyl-CoA, **C.** kanamycin A with AAC(6')-APH(2")(NHis) (Int-pET19b-pps) and acetyl-CoA, **D.** kanamycin A with AAC(6')-APH(2")(NHis) (Int-pET19b-pps) and *n*-propionyl-CoA, **E.** kanamycin A with AAC(6')-APH(2")(NHis) (pET28a) and acetyl-CoA, **F.** kanamycin A with AAC(6')-APH(2")(NHis) (pET28a) and *n*-propionyl-CoA, **G.** kanamycin A with AAC(6')-APH(2")(no tag) (Int-pET19b-pps) and acetyl-CoA, **H.** kanamycin A with AAC(6')-APH(2")(no tag) (Int-pET19b-pps) and *n*-propionyl-CoA, **I.** neomycin B with AAC(6')-APH(2")(CHis) (pET22b) and acetyl-CoA, and **J.** neomycin B with AAC(6')-APH(2")(CHis) (pET22b) and *n*-propionyl-CoA.

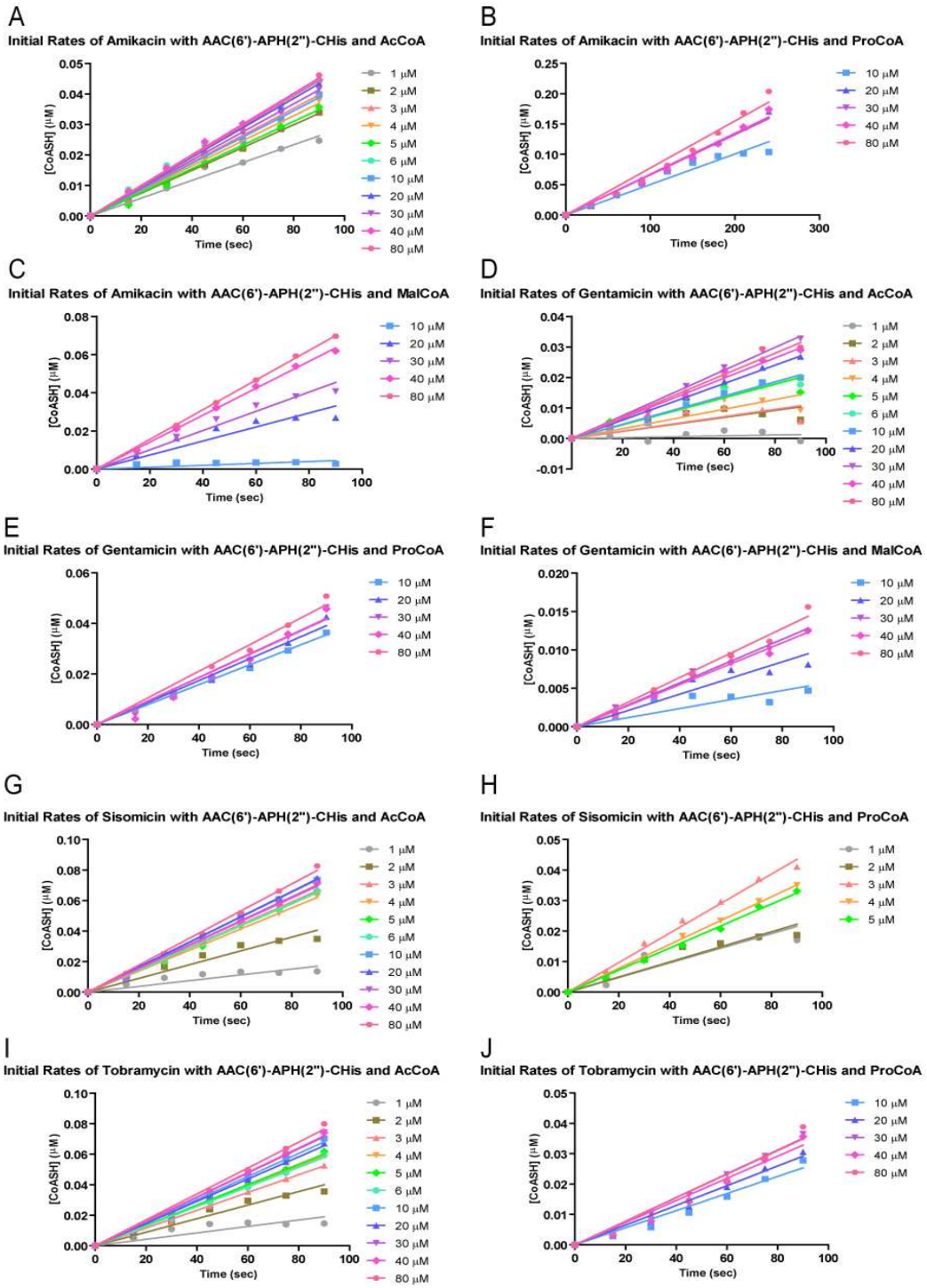

Figure S12. Example kinetic initial rates of **A.** amikacin with AAC(6')-APH(2")(CHis) (pET22b) and acetyl-CoA, **B.** amikacin with AAC(6')-APH(2")(CHis) (pET22b) and *n*-propionyl-CoA, **C.** amikacin with AAC(6')-APH(2")(CHis) (pET22b) and malonyl-CoA, **D.** gentamycin with AAC(6')-APH(2")(CHis) (pET22b) and acetyl-CoA, **E.** gentamicin with AAC(6')-APH(2")(CHis) (pET22b) and *n*-propionyl-CoA, **F.** gentamicin with AAC(6')-APH(2")(CHis) (pET22b) and malonyl-CoA, **G.** sisomicin with AAC(6')-APH(2")(CHis) (pET22b) and acetyl-CoA, **H.** sisomicin with AAC(6')-APH(2")(CHis) (pET22b) and *n*-propionyl-CoA, **I.** tobramycin with AAC(6')-APH(2")(CHis) (pET22b) and acetyl-CoA, and **J.** tobramycin with AAC(6')-APH(2")(CHis) (pET22b) and *n*-propionyl-CoA.

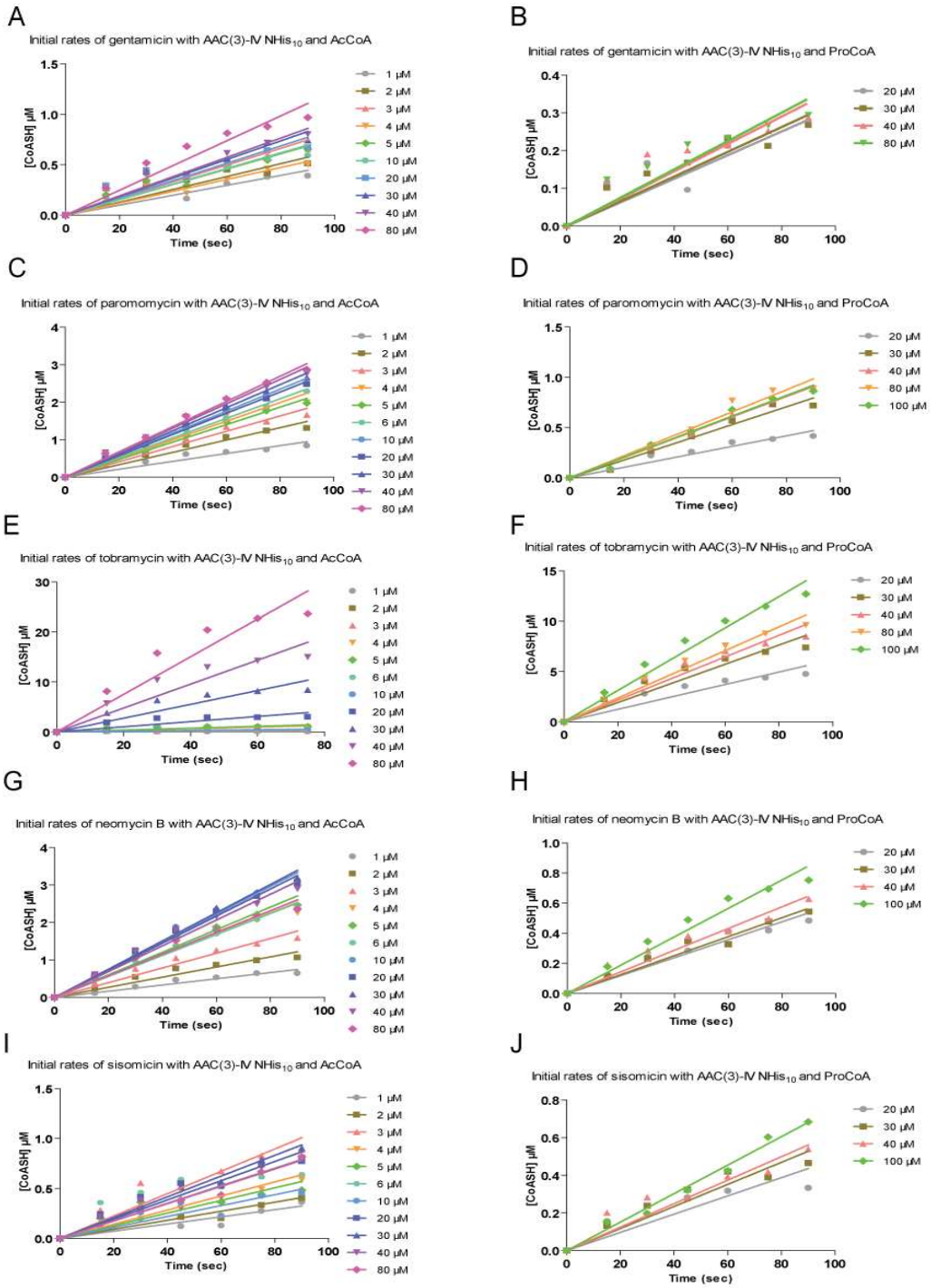

Figure S13. Example kinetic initial rates of **A.** gentamicin with AAC(3)-IV(NHis) (Int-pET19b-pps) and acetyl-CoA, **B.** gentamicin with AAC(3)-IV(NHis) (Int-pET19b-pps) and *n*-propionyl-CoA, **C.** paromomycin with AAC(3)-IV(NHis) (Int-pET19b-pps) and acetyl-CoA, **D.** paromomycin with AAC(3)-IV(NHis) (Int-pET19b-pps) and *n*-propionyl-CoA, **E.** tobramycin with AAC(3)-IV(NHis) (Int-pET19b-pps) and acetyl-CoA, **F.** tobramycin with AAC(3)-IV(NHis) (Int-pET19b-pps) and *n*-propionyl-CoA, **G.** neomycin B with AAC(3)-IV(NHis) (Int-pET19b-pps) and acetyl-CoA, **H.** neomycin B with AAC(3)-IV(NHis) (Int-pET19b-pps) and *n*-propionyl-CoA, **I.** sisomicin with AAC(3)-IV(NHis) (Int-pET19b-pps) and acetyl-CoA, and **J.** sisomicin with AAC(3)-IV(NHis) (Int-pET19b-pps) and *n*-propionyl-CoA.

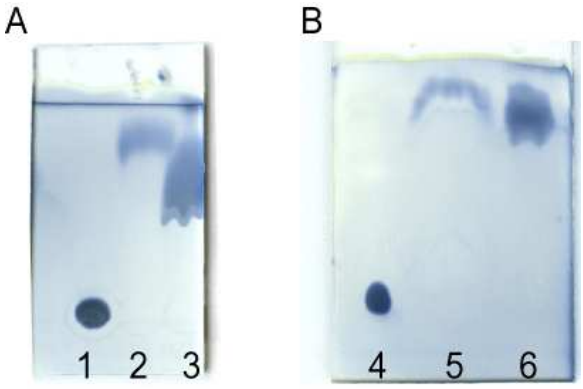

Figure S14. TLC visualization of AAC reaction starting materials and byproduct **A.** neomycin B (R_f = 0.23) (lane 1), acetyl-CoA (R_f = 0.91) (lane 2), and CoASH (R_f = 0.71) (lane 3) using a solvent system of 3:2/MeOH:NH_4OH, and **B.** gentamicin (R_f = 0.28) (lane 4), acetyl-CoA (R_f = 0.95) (lane 5), and CoASH (R_f = 0.85) (lane 6) using 6:1/MeOH:NH_4OH as the solvent system.

References

[1] T. Biswas, O. V. Tsodikov, *Febs J* **2008**, *275*, 3064.

[2] S. S. Hegde, F. Javid-Majd, J. S. Blanchard, *J Biol Chem* **2001**, *276*, 45876.

[3] B. Ostash, A. Saghatelian, S. Walker, *Chem Biol* **2007**, *14*, 257.